Desalination and Water Treatment
www.deswater.com

doi: 10.5004/dwt.2017.21679

97 (2017) 94–108
November

Opportunities of improvement of the MED seawater desalination process by pretreatments allowing high-temperature operation

Bartolomé Ortega-Delgado[a,b,*], Lourdes García-Rodríguez[c], Diego-César Alarcón-Padilla[a]

[a]*CIEMAT-Plataforma Solar de Almería, Ctra. de Senés s/n, 04200 Tabernas (Almería), Spain, Tel. +34 950 387800 Ext. 973; Fax: +34 950 365015; emails: bartolome.ortegadelgado@unipa.it (B. Ortega-Delgado), diego.alarcon@psa.es (D.C. Alarcón-Padilla)*
[b]*Dipartimento di Ingegneria dell'Innovazione Industriale e Digitale, Università degli Studi di Palermo, Viale delle Scienze, Ed.6., 90128 Palermo, Italy*
[c]*Department of Energy Engineering, Seville University, Escuela Técnica Superior de Ingeniería, Camino de los Descubrimientos s/n, 41092 Sevilla, Spain, Tel. +34 954 487231; Fax: +34 954 487233; email: mgarcia17@us.es*

Received 30 June 2017; Accepted 14 November 2017

ABSTRACT

In this work, the effect of increasing the top brine temperature (TBT) in a multi-effect distillation (MED) process and its influence on the main design and operational parameters, as gain output ratio (GOR) and specific heat transfer area is investigated. To that end, a detailed and advanced steady-state mathematical model for MED process with forward feed arrangement is developed and validated against data found in the literature. First, a comprehensive sensitivity analysis including key design parameters is carried out. The model is then used to simulate three different heating steam temperatures of 70°C, 100°C and 120°C with a variable number of effects between 9 and 34 and mean temperature difference between effects within 2°C–4°C. Results showed that, given a mean temperature difference between effects, the simultaneous increase in the number of effects and heating steam temperature leads to a significant improvement of the GOR, and a reduction of the specific heat transfer area. Particularly, for a mean difference of temperature between effects of 2.5°C, if the heating steam temperature is increased from 70°C to 120°C, the GOR is improved about 70%, the specific heat transfer area is reduced a 11% and the specific thermal energy consumption a 45%. This analysis provides meaningful results for the preliminary design of MED plants with high-temperature operation.

Keywords: Desalination; Multi-effect distillation; Forward feed; Nanofiltration; High temperature; Modelling

1. Introduction

Despite of the current dominance of the reverse osmosis (RO) technology in the seawater desalination market, thermal processes such as multi-effect distillation (MED) still have room for improvement, particularly in applications dealing with harsh waters or high fresh water purity requirements. However, the higher energy consumption of the MED process in comparison with the RO option constitutes one of the main drawbacks of this technology. The water productivity (kg of fresh water produced per kg of heating steam) of this system can be further increased by elevating the top brine temperature (TBT), which is typically limited by the salts precipitation (scale formation) in the surface of the heat exchangers, mainly calcium carbonate, magnesium hydroxide and calcium sulphate [1]. On the other hand, the use of membrane processes such as RO also present problems of scaling and fouling in the membranes, associated with high levels of total dissolved solids (TDS) in the intake seawater, which reduces the permeate production [2]. Hence, different pretreatment processes have been proposed in order to permit reduction in the energy consumption, limit the scale

* Corresponding author.

formation and eliminate the technical constraints intrinsically related to those technologies. One method already tested in commercial desalination plants is the nanofiltration (NF) pretreatment of the raw seawater entering a RO, multi-stage flash (MSF) or MED process, which can retain bivalent cations Ca^{+2} and Mg^{+2} and as consequence to increase the heating steam temperature in the case of MED and MSF processes (and so the number of effects) without risk of scaling. This integration helps to remove the main commented limitations associated with the low recovery ratio, the maximum temperature of operation or high TDS levels.

Studies found in the literature including NF pretreatment for seawater desalination processes are scarce, despite its potential for reducing the energy consumption. Those benefits were first verified in a project developed by the Saline Water Conversion Corporation (SWCC) and Hassan et al. [2], where a NF unit was integrated into a RO and a MSF pilot plant. The same author patented the use of NF membranes in combination with MSF, RO and MED desalination processes and proposed different integration and hybridization arrangements [3]. As a result, it was observed that the use of NF pretreatment decreased the turbidity, microorganisms, ions responsible of scaling phenomena (Ca^{2+}, Mg^{2+}, SO_4^{2-}, etc.) and TDS from the intake seawater, which allowed to increase the recovery ratio up to 70%–80%, to rise the TBT to 120°C and to reduce the energy consumption between 25% and 30%. At commercial scale, the first NF system integrated into a MSF plant was proved to increase the capacity over 40% from the nominal value (from 22,700 to 32,800 m^3/d), project developed by Leading Edge Technologies Ltd. (LET), USA and Besix Consortium at UAE [4]. The TBT was raised from 105°C to 120°C approximately, with the respective increase in the capacity of the plant. In addition, the capital and operation costs were reduced, compared with the standalone systems. Hamed [5] reviewed hybrid desalination systems including membrane and thermal processes coupled to power plants. He pointed out the promising concept of NF pretreatment for the removal of the ions causing scale on the tubes of the evaporators. Tests carried out on a MSF pilot plant operating at a TBT of 130°C resulted successful, increasing the recovery ratio up to 70% with respect to 35% of normal MSF plants. Also, Zhou et al. [6] pointed out the benefits of introducing NF pretreatment into diverse seawater desalination technologies in order to reduce the costs associated with the scale formation. Particularly, if MED process is considered, the TBT could be raised up to 125°C without the risk of scaling. Moreover, the recovery ratio and water production could be improved.

Accordingly, the introduction of pretreatment processes for eliminating the risk of scaling in MED desalination technology and increasing the TBT would result in a significant improvement of the water productivity and reduction of the overall energy consumption. Particularly, the detailed analysis of the increment of the TBT in MED units and the influence on the main design and performance parameters is of great interest and suggested by the above-mentioned authors. It is worth highlighting that, among the different MED configurations, the forward feed is the most suitable one to investigate the augmentation of the maximum temperature of operation due to the lower risk of scaling (the maximum brine concentration is reached in the effect of lowest temperature) [7].

One of the first steady-state mathematical models found for MED process with forward feed (MED-FF) arrangement was developed by El Sayed and Silver [8], relying on simplified assumptions such as constant thermophysical properties of the seawater or equal heat rates on the evaporators. The effect of the vapour pressure losses caused by friction was accounted by augmenting the boiling point elevation (BPE). They obtained useful analytical expressions to calculate the performance ratio, the thermal loads and heat transfer surface areas. In addition, they considered preheaters and flash boxes in the system analysis. El-Dessouky et al. [9] developed a detailed mathematical model for MED-FF units, including preheaters and flash boxes. They assumed constant heat transfer areas in evaporators and preheaters, the influence of vapour leaks on the venting system and the effect of thermodynamic losses due to the BPE, non-equilibrium allowance (NEA) and vapour pressure drops through the demisters, connecting lines and during the condensation inside the tubes of the evaporators. Moreover, the thermophysical properties of the seawater were calculated as function of the temperature and salinity, and the effect of the non-condensable gases on the condensation heat transfer coefficients was accounted. They concluded that the thermal performance of the unit is nearly independent of the TBT (for a fixed number of effects) and significantly affected by the number of effects. Also, the overall heat transfer coefficients in evaporators and preheaters increased with the temperature, being higher for evaporators than for the preheaters (2.3-2.7 and 1.9-2.1 kW/(m^2 °C), respectively). Other steady-state mathematical model for MED-FF plants, based on mass and energy balances applied on the different components of the system, was presented by Mistry et al. [10]. They used a simultaneous equations solver, which provides more flexibility to the model as it does not require developing any algorithm to reach the convergence and at the same time reduces the number of assumptions. The model was compared with others found in the literature by simulating the gain output ratio (GOR) and specific heat transfer area (sA) as function of different operational variables. The results showed that the model agreed quite well with the one from El-Sayed and Silver [8], providing more details about the temperature profiles in the MED plant. Moreover, it had much simpler implementation and less assumptions that the model from El-Dessouky et al. [9]. However, only the BPE was considered in the calculation of the so-called thermodynamic losses, ignoring the saturation temperature losses due to the vapour pressure drops in the demisters, connecting lines and during the condensation inside the evaporators. Due to the fact that the specific heat transfer area is greatly affected by the saturation temperature losses of the generated vapour, from its generation in one effect to the condensation inside the evaporator of the following effect, they should be properly accounted while modelling MED plants. In addition, some approximations were done, such as neglecting the effect of the non-equilibrium allowance as a result of the flashing processes of the brine in the effects and the distillate in the flash boxes. The present model for MED-FF units takes advantage of the flexibility of a simultaneous equation solver while calculating in detail the saturation temperature losses, including BPE, non-equilibrium allowance and saturation temperature reduction of the vapour as consequence of the pressure drop in the demister, connecting lines and during the condensation inside the tubes of the evaporator.

The objective of this work is to investigate the effect of augmenting the TBT and number of effects in MED-FF units on the main design and operation parameters (GOR, specific heat transfer area and specific thermal energy consumption) and further improve the existing FF-MED models in the literature. Seawater pretreatments such as NF would permit to increase the TBT without the risk of scaling and fouling, by retaining the bivalent ions and rejecting the microorganisms. For that purpose, a detailed mathematical steady-state model of a MED with forward feed arrangement has been developed and validated against data found in the literature. This model includes some improvements with respect to others previously published, like the detailed calculation of the saturation temperature losses of the vapour. Also, a sensibility analysis regarding different design and operational parameters of the MED process (number of effects, terminal temperature difference in the first effect, brine salinity of the intake seawater, etc.) has been carried out.

2. Forward feed MED model

2.1. Process description

A MED system for seawater desalination is based on a sequence of evaporation and condensation processes taking place inside a train of connected vessels, called effects, each one at lower pressure and temperature than the previous. In essence, this system takes advantage of the enthalpy of condensation of the generated vapour in one effect for promoting a new evaporation process in the following effect, repeating the sequence up to the last effect.

Among the different feed arrangements of the MED system, the forward feed configuration is characterized by the equal direction of the vapour and feed flows in the system. Furthermore, the lowest salinity of the brine is reached in the first effect and is progressively increasing up to the last effect. Hence, this configuration is specially indicated for higher temperatures of the external heating steam as the risk of scale formation is minimized.

In this system, each effect is comprised of a horizontal tube falling film evaporator, a demister and a preheater, except the last one which does not have a preheater but a condenser, called end condenser (Fig. 1). The external thermal energy, usually saturated steam (heating steam) below 70°C to avoid the appearance of scaling in the tubes, is introduced exclusively in the evaporator of the first effect and represents the primary energy source which drives the entire distillation process. First, the seawater enters the system from intake beach wells or submarine pipelines. It is directed to the end condenser where is used to condense the vapour generated in the last effect. At the outlet of the end condenser, the seawater is divided into two streams: the feed seawater, which goes to the first effect passing through the preheaters of each effect, and the cooling seawater, which rejects the waste heat back to the sea. The preheating of the seawater permits to reduce the energy requirements of the process thanks to the condensation of a fraction of the total vapour generated in each effect. The feed seawater (feedwater), after being preheated, is sprayed over the tube bundle of the first evaporator where is partially evaporated due to the heat released by the condensation of the external vapour, which returns as saturated liquid to the steam generation source. From one side, vapour is produced, while the unevaporated brine remains at the bottom of the effect and constitutes the feedwater for the next effect. The vapour produced, considered free of salts, passes through a demister in order to retain the brine droplets, and is directed to a preheater where part of it condenses. The rest of the vapour is brought to the evaporator of the second effect and constitutes the driven force of the new evaporation process, at lower pressure and temperature. In this effect, the feedwater is the brine generated in the previous, which undergoes a flash process and produces additional vapour. Both the distillate produced in the preheater and inside the evaporator are collected in a flash box, producing additional flash vapour which is introduced in the vapour space of the effect. This process is repeated sequentially up to the last effect.

2.2. Mathematical model

A steady-state mathematical model for a FF-MED process is developed by applying the mass and energy balance equations over the components of the plant, together with the heat transfer equations associated with the heat exchangers (evaporators, preheaters and end condenser). The generic

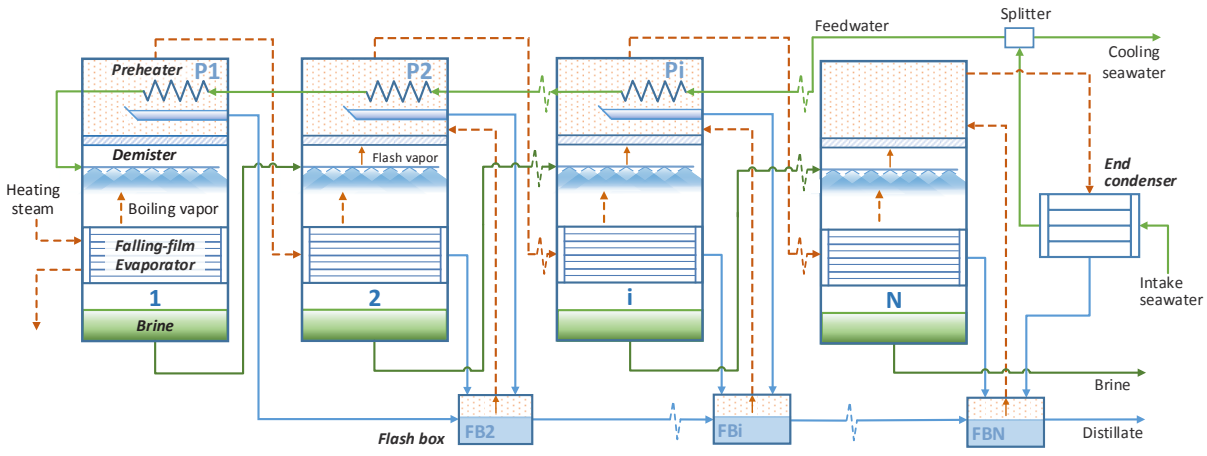

Fig. 1. Schematic diagram of a multi-effect distillation unit with forward feed arrangement.

FF-MED system includes N effects, N – 1 preheaters and N – 1 distillate flashing boxes (Fig. 1). By default, the input variables needed to solve the model are the following: the temperature of the heating steam, T_s; the temperature and salinity of the seawater intake, T_{in} and X_{in}, respectively; the temperature and salinity of the brine in the last effect, T_N and X_N, respectively; the temperature of the cooling seawater, T_F; the minimum temperature difference in the end condenser, TTD_c and preheater 1, TTD_{preh1}; and the geometric and physical characteristics of the demister, connecting lines and evaporator tubes.

For the implementation of the FF-MED model, Engineering Equation Solver (EES) software has been used [11], which solves simultaneously all the nonlinear equations set in the system (using the Newton-Raphson method). This software is useful for the characterization of thermal systems similar to the one studied here because it includes libraries for determining the thermophysical properties of numerous substances, included pure water (IAPWS Formulation 1995 [12]) and seawater (Sharqawy et al. [13]). Moreover, it does not need to create an algorithm to sequentially solve the equations, providing more degrees of freedom. On the other hand, the convergence is strongly subject to proper initial guesses and a reasonable range of variation of the variables.

In the development of the model, the following approximations have been taken into account:

- Constant and equal heat transfer areas in evaporators and preheaters. This is a common practice in the real thermal desalination industry due to economic reasons.
- The thermophysical properties of the seawater are function of the temperature and salinity.
- The distillate produced is considered salt-free.
- The thermal losses to the environment are neglected as the equipment is supposed to be well insulated and the operation temperatures are relatively low (40°C-120°C).
- The temperature of the vapour is considered equal to the brine temperature in each effect. That means that the vapour is slightly superheated by the BPE.
- In each evaporator, both the inlet steam and the exiting condensed liquid are supposed to be in saturation conditions.
- The variables habitually known as thermodynamic losses have been fully implemented: the BPE, the non-equilibrium allowance in the effects and flashing boxes, and the saturation temperature decrease of the vapour due to the pressure losses in the demister, connecting lines and during the condensation inside the evaporators.
- The vapour suffers an isenthalpic process while passing through the demister.
- The temperature of the flashing vapour in the flash box is equal to the temperature in the vapour space of the effect.
- Due to the utilization of a vacuum system, no vapour leaks have been considered.

2.2.1. Global mass and salt balances

The global mass and salinity balance applied to the complete system (Fig. 1) leads to:

$$q_F = q_D + q_B \tag{1}$$

$$q_F X_F = q_B X_N \tag{2}$$

where q_F is the mass flow rate of feed seawater going into the first effect, q_D is the total mass flow rate of distillate produced, q_B is the mass flow rate of brine exiting the last effect, X_F is the salinity of the feed seawater and X_N is the salinity of the brine in the last effect. Notice that as local mass balances have been applied in the effects, the global mass balance is only for verification purposes. Similarly, the global salinity balance is equivalent to the salinity balance in the last effect.

The total mass flow rate of distillate generated in the plant is the sum of the mass flow rate of vapour produced by boiling in each effect q_{Di} plus the vapour produced by flashing q_{FEi} (except in the first effect where there is not flashing phenomena):

$$q_D = \sum_{i=1}^{N} q_{Di} + \sum_{i=2}^{N} q_{FEi} \tag{3}$$

2.2.2. Temperature profiles

The temperature of the brine in a generic effect i is equal to the saturation temperature of the vapour formed by boiling plus the BPE, which takes into account the presence of salts in the water:

$$T_i = T_{Vsat,i} + BPE_i \tag{4}$$

The BPE is obtained with the correlation proposed by Sharqawy et al. [13], which is function of the temperature and salinity of the brine.

Also the temperature of the brine and the temperature of the vapour in each effect are considered equal:

$$T_i = T_{V_i} \tag{5}$$

It is supposed that the vapour suffers an isenthalpic process through the demisters, reaching a temperature T'_{Vi} in the vapour space, with the respective pressure drop. The saturation temperature of the generated vapour decreases in the path to the next evaporator, because of the pressure drop in the demister, the connecting lines and the condensation inside the tubes. This temperature drop causes a decrease in the temperature difference between effects, which is the driven force of the process. Therefore, the condensation temperature of the vapour generated in the effect i, which takes place inside the evaporator of the effect i + 1, from i = 1 to N – 1, is obtained with:

$$T_{c,i} = T_{Vi} - BPE_i - \left(\Delta T_{m,i} + \Delta T_{l,i} + \Delta T_{c,i}\right) \tag{6}$$

where $\Delta T_{m,i}$, $\Delta T_{l,i}$ and $\Delta T_{c,i}$ are the saturation temperature drops in the demister, connecting lines and condensation process, all referred to the effect i and starting from the second effect. Notice that the condensation temperature in the first evaporator is the saturation temperature of the heating steam and the corresponding condensation temperature of the effect i + 1 is $T_{c,i}$, from i = 1 to N – 1.

The decrease in the saturation temperature of the vapour after passing through the demister of a generic effect i is the difference between the saturation temperatures of the vapour be($T_{\mathrm{Vsat},i}$ and $T'_{\mathrm{Vsat},i}$, respectively). Similarly, the saturation temperature drop occurring in the connecting lines between the effect i and effect $i+1$ is equal to $T'_{\mathrm{Vsat},i}$ minus the saturation temperature of the vapour at the inlet of the following evaporator ($T'_{c,i}$). Lastly, the saturation temperature losses of the vapour during the condensation in the tube bundle are defined as the difference between $T'_{c,i}$ and the condensation temperature ($T_{c,i}$).

$$\Delta T_{m,i} = T_{\mathrm{Vsat},i} - T'_{\mathrm{Vsat},i} \tag{7}$$

$$\Delta T_{l,i} = T'_{\mathrm{Vsat},i} - T'_{c,i} \tag{8}$$

$$\Delta T_{c,i} = T'_{c,i} - T_{c,i} \tag{9}$$

The mentioned temperatures are calculated with the pressure drops of the formed vapour while flowing to the tubes of the next evaporator. Particularly, the pressure decrease in the demister is obtained with the correlation proposed by El-Dessouky and Ettouney [14]. For the pressure drop in the connecting lines, due to the friction with the walls, the Unwin's formula [15] has been used. Finally, the pressure drop due to the condensation of the vapour inside the tubes of the evaporator has been determined by means of the methodology described in ESDU [16], which relies on the Friedel's correlation [17].

2.2.3. First effect

The first effect is different from the rest of the MED unit as is the place where the external energy is introduced (Fig. 2). The mass balance applied to a control volume (CV) containing the first effect provides:

$$q_F = q_{B1} + q_{T1} \tag{10}$$

where q_{B1} is the mass flow rate of brine exiting the first effect and q_{T1} is the total mass flow rate of vapour generated within the first effect, which in this case is only the one produced by boiling (q_{D1}). Notice that in this effect the seawater introduced does not suffer a flash process because its temperature is below the saturation temperature at the existing pressure inside the effect.

The salinity balance applied to the same CV is shown below, where it has been assumed that the vapour generated is free of salts:

$$q_F X_F = q_{B1} X_1 \tag{11}$$

with q_{B1} and X_1 are the mass flow rate and salinity of the brine in the effect 1, respectively.

Finally, the energy balance in this first effect, considering all the streams entering and exiting the CV, is as follows:

$$q_s \lambda_s + q_F h_{\mathrm{preh2}} = (1-\alpha_1) q_{T1} h'_{V1} + \alpha_1 q_{T1} h'_{C1} + q_{B1} h_{B1} \tag{12}$$

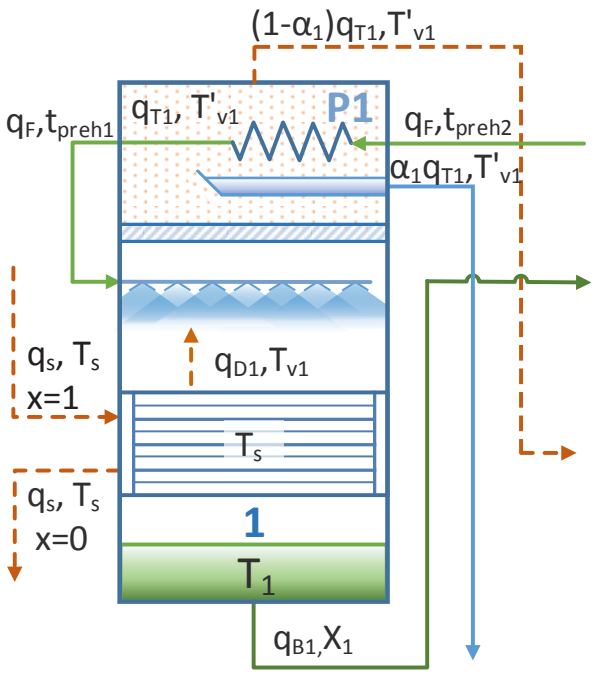

Fig. 2. Schematic diagram of the first effect.

where q_s is the mass flow rate of the external heating steam; λ_s is the specific enthalpy of condensation of the heating steam at T_s; h_{preh2} is the specific enthalpy of the feed seawater before entering the first preheater, at t_{preh2}; α_1 is the fraction of the total steam that condenses in the first preheater; h'_{V1} is the specific enthalpy of the steam in the vapour space at T'_{V1}, after passing through the demister; h'_{C1} is the specific enthalpy of the condensate in the preheater at T'_{V1} and h_{B1} is the specific enthalpy of the brine at the bottom of the effect at T_1.

The area of the evaporator is obtained by applying the heat transfer equation in this component. The rate of heat transfer (Q_1) that takes place between the condensing steam and the sprayed seawater in this first evaporator accounts both for the sensible and latent heat added:

$$Q_1 = q_F \bar{c}_{p1} (T_1 - t_{\mathrm{preh1}}) + q_{D1} \lambda_{V1} = A_1 U_{e1} (T_s - T_1) \tag{13}$$

where $\bar{c}_{p1}$ is the specific heat at constant pressure of the feedwater between T_1 and t_{preh1}, t_{preh1} is the temperature of the feedwater after passing through the preheater associated with the first effect, q_{D1} is the mass flow rate of vapour produced by boiling in the first effect, λ_{V1} is the specific enthalpy of evaporation of the water at $T_{\mathrm{Vsat},1}$, A_1 is the heat transfer area of the evaporator and U_{e1} is the overall heat transfer coefficient of the evaporator, which is calculated using the correlation proposed by El-Dessouky and Ettouney [18] as function of the temperature:

$$U_{e1} = 1.9695 + 1.2057 \cdot 10^{-2} T_1 - 8.5989 \cdot 10^{-5} T_1^2 + 2.5651 \cdot 10^{-7} T_1^3 \tag{14}$$

2.2.4. Effects from 2 to N – 1

The mass balance applied to the CV defined by the generic effect *i* (Fig. 3) is as follows:

$$q_{\mathrm{Bi}} = q_{B,i-1} - q_{\mathrm{Di}} - q_{\mathrm{FEi}} \tag{15}$$

being q_{Bi} and $q_{B,i-1}$ the mass flow rates of the brine exiting and entering the effect *i*, respectively.

Similarly, the salt balance in the CV establishes that:

$$q_F X_F = q_{\mathrm{Bi}} X_i \tag{16}$$

where q_{Bi} and X_i are the mass flow rate and salinity of the brine in the effect *i*.

The energy balance applied to the same CV gives:

$$\begin{aligned}&(1-\alpha_{i-1})q_{T,i-1}\lambda_{c,i-1} + q_{\mathrm{FBi}}h''_{\mathrm{Vi}} + q_{B,i-1}h_{B,i-1}\\ &= (1-\alpha_i)q_{\mathrm{Ti}}h'_{\mathrm{Vi}} + \alpha_i q_{\mathrm{Ti}}h'_{\mathrm{ci}} + q_F\bar{c}_{p,\mathrm{preh},i}\left(t_{\mathrm{preh},i} - t_{\mathrm{preh},i+1}\right) + q_{\mathrm{Bi}}h_{\mathrm{Bi}}\end{aligned} \tag{17}$$

where α_i is the fraction of vapour condensed in the preheater *i*; $\lambda_{c,i-1}$ is the specific enthalpy of condensation of the vapour inside the evaporator of the effect *i*, at $T_{c,i-1}$; q_{FBi} is the mass flow rate of vapour produced by flash in the flash box *i*; h''_{Vi} is the specific enthalpy of the flashing vapour at T''_{Vi}; $\varepsilon_{\mathrm{preh},i}$ is the specific heat of the feed water at constant pressure and mean temperature between $t_{\mathrm{preh},i}$ and $t_{\mathrm{preh},i+1}$ and q_{Ti} is the total mass flow rate of vapour produced by boiling within the effect (q_{Di}), by flashing of the brine (q_{FEi}) and by flashing of the distillate (q_{FEi}):

$$q_{\mathrm{Ti}} = q_{\mathrm{Di}} + q_{\mathrm{FEi}} + q_{\mathrm{FBi}} \tag{18}$$

In the effects from 2 to *N*, the brine entering the effects suffers a flashing process because of being slightly superheated and discharged into a lower pressure effect. This process is described with the following balance:

$$q_{\mathrm{FEi}}\lambda_{\mathrm{FEi}} = q_{B,i-1}\bar{c}_{p,\mathrm{FEi}}\left(T_{i-1} - T_{B,\mathrm{FEi}}\right) \tag{19}$$

where λ_{FEi} is the specific enthalpy of evaporation of the seawater at T_i, $\bar{c}_{p,\mathrm{FEi}}$ is the specific heat at constant pressure and mean temperature between T_{i-1} and $T_{B,\mathrm{FEi}}$, with $T_{B,\mathrm{FEi}}$ the temperature of the unevaporated brine in the effect *i* after the flashing process. The temperature of the brine is higher than the boiling temperature T_i by the non-equilibrium allowance, which represents the deviation of the real process with respect to the ideal one in equilibrium. This variation is mainly caused by the finite time period in which the flash process occurs [19]. For that reason the equilibrium conditions between the liquid and the vapour cannot be reached and the temperature of the resulting brine is higher than the temperature in the equilibrium.

$$T_{B,\mathrm{FEi}} = T_i + \mathrm{NEA}_i \tag{20}$$

where the NEA_i is calculated by means of the correlation published by Miyatake et al. [20] as function of the temperature difference (ΔT_i) of the boiling brine in the effects *i* –1 and *i*:

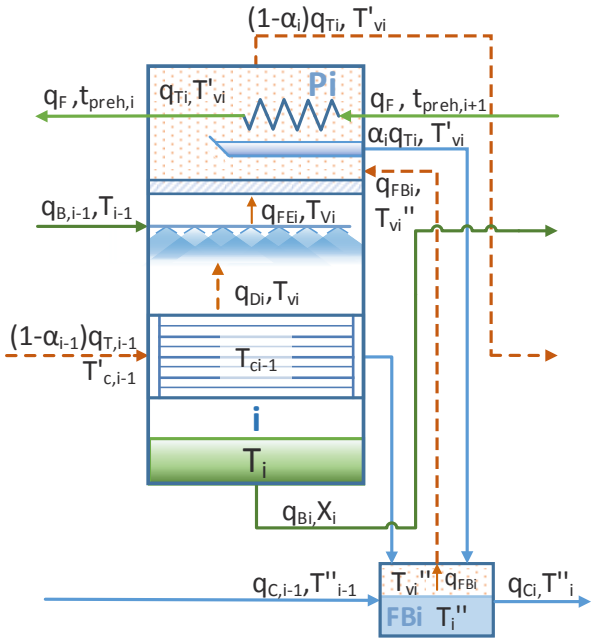

Fig. 3. Schematic diagram of the generic effect *i*.

$$\mathrm{NEA}_i = \frac{33\left(\Delta T_i\right)^{0.55}}{T_{\mathrm{Vi}}} \tag{21}$$

The validity of this correlation is somehow limited to the experimental conditions considered in the work of these authors. Particularly, they obtained data from flash evaporation experiments carried out in a pool of pure water, inside a chamber of 40 cm high and a diameter of 8 cm.

The heat transfer areas of the evaporators (from 2 to *N* – 1) are obtained with the heat transfer equations related to the condensation-evaporation process that takes place in the tube bundle at constant temperature:

$$Q_i = (1-\alpha_{i-1})q_{\mathrm{Ti}}\lambda_{c,i-1} = A_i U_{\mathrm{ei}}\left(T_{c,i-1} - T_i\right) \tag{22}$$

where Q_i is the rate of heat transfer and U_{ei} is the overall heat transfer coefficient in the evaporator *i*, determined using Eq. (14) with the corresponding temperature.

2.2.5. Last effect

The mass balance in the last effect (Fig. 4) establishes that the brine coming from the previous effect ($q_{B,N-1}$) is equal to the mass flow rate of vapour generated by flash ($q_{\mathrm{FE},N}$) plus the mass flow rate of vapour generated by boiling (q_{DN}) and the unevaporated brine remaining at the bottom of the effect (q_{BN}). This equation is expressed as follows:

$$q_{B,N-1} = q_{\mathrm{FE},N} + q_{\mathrm{DN}} + q_{\mathrm{BN}} \tag{23}$$

The energy balance in this effect is different from the rest because of its particular configuration. There is no preheater associated with this effect and all the vapour generated is driven to the end condenser where it releases its latent heat

to the intake seawater. The condensate generated here is collected in the last flash box.

$$\left(1-\alpha_{N-1}\right)q_{T,N-1}\lambda_{c,N-1}+q_{\mathrm{FB},N}h_{\mathrm{VN}}^{''}+q_{B,N-1}h_{B,N-1}=q_{\mathrm{TN}}h_{\mathrm{VN}}^{'}+q_{\mathrm{BN}}h_{\mathrm{BN}} \quad (24)$$

In addition, part of the vapour is produced by flash of the incoming brine:

$$q_{\mathrm{FE},N}\lambda_{\mathrm{FE},N}=q_{B,N-1}\bar{c}_{p,\mathrm{FEN}}\left(T_{N-1}-T_{B,\mathrm{FEN}}\right) \quad (25)$$

The temperature of the unevaporated brine, $T_{B,\mathrm{FEN}}$, is obtained with the NEA_N:

$$T_{B,\mathrm{FEN}}=T_N+\mathrm{NEA}_N \quad (26)$$

Finally, the heat transfer equation associated with the evaporator of this last effect is as follows:

$$Q_N=\left(1-\alpha_{N-1}\right)q_{T,N-1}\lambda_{c,N-1}=A_N U_{\mathrm{eN}}\left(T_{c,N-1}-T_N\right) \quad (27)$$

2.2.6. End condenser

In the end condenser, the vapour generated in the last effect condenses and warms up the intake seawater (Fig. 4). Part of the seawater at the outlet of the end condenser (rejected cooling seawater) is sent back to the sea in order to reject the excess of heat not used in the process. The mass balance in the splitter and the energy balance applied in the end condenser are expressed, respectively, by:

$$q_{\mathrm{in}}=q_F+q_{\mathrm{cw}} \quad (28)$$

$$q_{\mathrm{in}}\left(h_F-h_{\mathrm{in}}\right)=q_{\mathrm{TN}}\lambda_c \quad (29)$$

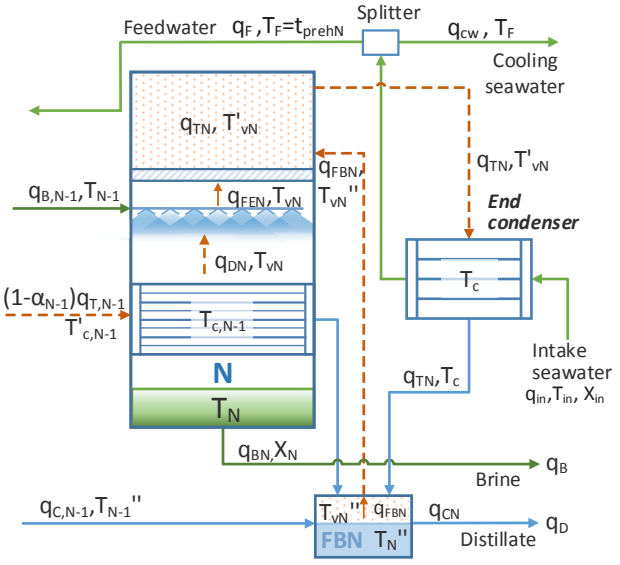

Fig. 4. Schematic diagram of the last effect and end condenser.

where q_{in} is the mass flow rate of intake seawater entering the end condenser; q_{cw} is the mass flow rate of cooling seawater; h_F is the specific enthalpy of the seawater at T_F after passing through the end condenser; h_{in} is the specific enthalpy of the intake seawater at T_{in} and λ_c is the specific enthalpy of condensation of the vapour coming from the last effect, at T_c.

The heat transfer equation applied to the end condenser, which is a shell and tube heat exchanger that can be assumed as counter-flow, is defined below:

$$Q_c=A_c U_c \mathrm{LMTD}_c=U_c A_c\frac{\Delta T_{\mathrm{in}}^c-\Delta T_{\mathrm{out}}^c}{\ln\left(\frac{\Delta T_{\mathrm{in}}^c}{\Delta T_{\mathrm{out}}^c}\right)}=U_c A_c\frac{T_F-T_{\mathrm{in}}}{\ln\left(\frac{T_c-T_{\mathrm{in}}}{T_c-T_F}\right)} \quad (30)$$

where A_c is the heat transfer area of the condenser, U_c is the overall heat transfer coefficient related to the end condenser and obtained using the correlation proposed by El-Dessouky and Ettouney [18]:

$$U_c=1.7194+3.2063\cdot10^{-3}T_c+1.5971\cdot10^{-5}T_c^2-1.9918\cdot10^{-7}T_c^3 \quad (31)$$

and LMTD_c is the log mean temperature difference of the condenser, defined as function of the temperatures differences at the inlet ($\Delta T_{\mathrm{in}}^c=T_c-T_{\mathrm{in}}$) and at the outlet of the condenser ($\Delta T_{\mathrm{out}}^c=T_c-T_F$).

2.2.7. Preheaters

Each of the $N-1$ preheaters is thermodynamically defined by applying an energy balance over a CV containing them and with the heat transfer equation associated to the heat transfer process. It is assumed that the BPE of the generated vapour is released in the preheaters. Thus, the energy balance considers both latent and sensible heat transfer, and is established as follows:

$$q_F\bar{c}_{p,\mathrm{preh},i}\left(t_{\mathrm{preh},i}-t_{\mathrm{preh},i+1}\right)=\alpha_i q_{\mathrm{Ti}}\lambda_{\mathrm{Vi}}^{'}+\alpha_i q_{\mathrm{Ti}}\bar{c}_{p,\mathrm{BPEi}}\left(T_{\mathrm{Vi}}^{'}-T_{\mathrm{Vsat},i}^{'}\right) \quad (32)$$

where $\bar{c}_{p,\mathrm{preh,i}}$ is the specific heat of the seawater at constant pressure and mean temperature between $t_{\mathrm{preh},i}$ and $t_{\mathrm{preh},i+1}$, $t_{\mathrm{preh},i}$ and $t_{\mathrm{preh},i+1}$ are the temperatures of the seawater at the outlet and the inlet of the preheater i, respectively, and $\bar{c}_{p,\mathrm{BPEi}}$ is the specific heat of the vapour at constant pressure and mean temperature between T'_{Vi} and $T'_{\mathrm{Vsat},i}$.

The heat transfer equations associated with the preheaters are defined below, formed similarly to the case of end condenser:

$$Q_{\mathrm{preh},i}=A_{\mathrm{preh},i}U_{\mathrm{preh},i}\mathrm{LMTD}_{\mathrm{preh},i}=U_{\mathrm{preh},i}A_{\mathrm{preh},i}\frac{t_{\mathrm{preh},i}-t_{\mathrm{preh},i+1}}{\ln\left(\frac{T_{\mathrm{Vi}}^{'}-t_{\mathrm{preh},i+1}}{T_{\mathrm{Vi}}^{'}-t_{\mathrm{preh},i}}\right)} \quad (33)$$

where $A_{\mathrm{preh},i}$ is the heat exchanger area, $U_{\mathrm{preh},i}$ is the overall heat transfer coefficient and $\mathrm{LMTD}_{\mathrm{preh},i}$ is the log mean temperature difference, referred to a generic preheater i, from $i=1$ to $N-1$. Notice that in Eq. (33) the effect of the sensible heat of the vapour (superheated by the BPE) has been neglected

when compared with the specific heat of condensation, for simplicity. Moreover, the overall heat transfer coefficient has been calculated using the same expression that for the end condenser case.

2.2.8. Flash boxes

The flash boxes are used to collect the distillate generated in the preheaters and evaporators and to produce additional flash vapour (Fig. 3). In this work, it has been assumed that the vapour temperatures inside the flash boxes (T'_{Vi}) are equal to those of the vapour space in the effects, after the demisters (T'_{Vi}), as they are interconnected. Therefore, the condensate suffers a sudden flash process due to its saturated condition and the decrease in the pressure. The temperature of the distillate (T''_i) is then higher than the temperature of the vapour in the flash box by the non-equilibrium allowance (NEA''):

$$T''_i = T''_{Vi} + \mathrm{NEA}''_i \quad \text{with} \quad i = 2..N \tag{34}$$

where NEA''_i is obtained with the correlation of Eq. (21) adapted to the flash boxes:

$$\mathrm{NEA}''_i = \frac{33\left(T_{c,i-1} - T''_i\right)^{0.55}}{T''_{Vi}} \tag{35}$$

There are $N - 1$ flash boxes, which has been numbered starting from the second. The mass balances applied in the flash boxes are as follows, where for $i = 1$ the equation provides the definition of q_{C1}:

$$q_{Ci} = \sum_{k=1}^{i-1} q_{T,k} + \alpha_i q_{Ti} - \sum_{j=2}^{i} q_{FB,j} \quad \text{with} \quad i = 1..N-1 \tag{36}$$

where q_{Ci} is the mass flow rate of the distillate collected in the flash box i at T''_i . In the last flash box the mass balance is:

$$q_{CN} = q_{C,N-1} + \left(1 - \alpha_{N-1}\right) q_{T,N-1} + q_{TN} - q_{FB,N} \tag{37}$$

The energy balances in the flash boxes for are presented below, from $i = 2$ to $N - 1$:

$$q_{C,i-1} h''_{c,i-1} + \left(1 - \alpha_{i-1}\right) q_{T,i-1} h_{c,i-1} + \alpha_i q_{Ti} h'_{ci} = q_{FBi} h''_{Vi} + q_{Ci} h''_{ci} \tag{38}$$

where $h''_{c1} = h'_{c1}$. Finally, the energy balance applied in the last flash box gives:

$$q_{C,N-1} h''_{c,N-1} + \left(1 - \alpha_{N-1}\right) q_{T,N-1} h_{c,N-1} + q_{TN} h_{cN} = q_{FBN} h''_{VN} + q_{CN} h''_{cN} \tag{39}$$

2.3. Main parameters characterizing the MED system

One variable frequently used to measure the productivity of a MED process is the GOR, defined as the ratio of distillate mass flow rate (q_D) produced to the heating steam mass flow rate (q_s) introduced in the first evaporator:

$$\mathrm{GOR} = \frac{q_D}{q_s} \tag{40}$$

Other significant parameter related to the capital cost of the MED plant is the specific heat transfer area (sA), which is defined as the sum of all the heat exchanger surface areas (evaporators, preheaters and end condenser) divided by the overall distillate mass flow rate:

$$\mathrm{sA} = \frac{\sum_{i=1}^{N} A_i + \sum_{i=1}^{N-1} A_{\mathrm{preh},i} + A_c}{q_D} \tag{41}$$

The specific thermal energy consumption (sE) is also used to quantify the thermal efficiency of a MED, which is defined as the mass flow rate of heating steam times the specific enthalpy of condensation of the steam divided by the mass flow rate of distillate produced, with the corresponding conversion factors, in kWh/m^3.

$$\mathrm{sE} = \frac{q_s \lambda_s}{q_D / \rho_D} \cdot \frac{1}{3600} \tag{42}$$

3. Validation of the FF-MED model and sensitivity analysis

3.1. Validation of the model

The developed model is compared with others obtained from the literature in order to validate it. In general, the present model is similar to the one described by El-Dessouky et al. [9] and shares some of its features. However, some differences can be observed. The most important difference is the programming method chosen for the implementation of the model, from which derives a simpler coding and higher flexibility in the simulations. As commented before, a simultaneous equation solver system was selected, contrary to the sequential solving taken by El-Dessouky et al. [9], just as the model presented by Mistry et al. [10]. Also, the present model considers a preheater associated with the first effect, which is not accounted in the model developed by El-Dessouky et al. [9]. In addition, in this model the amount of vapour condensed in the preheaters is a fraction α of the total vapour produced by boiling and flash, while in the latter only the flash vapour is considered to be condensed in the preheaters. On the contrary, the model developed by El-Dessouky et al. [9] accounts for the presence of non-condensable gases and vapour leakages, which is not considered here. A list with the differences with other models presented in the selected literature is shown in Table 1.

For the validation of the MED-FF model, results from Mistry et al. [10] have been taken. Particularly, the variation of the GOR and sA with the number of effects and heating steam temperature was considered. To perform the comparison, the same specifications for the MED were selected and presented in Table 2. The model has been calibrated by minimizing the thermodynamic losses: only the demister of the first effect has been taken into account and the diameters of the connecting lines and the tubes of the evaporators has been selected large enough in order to decrease the friction losses.

Table 1
Comparison between the assumptions of the selected forward feed MED models

Parameter	El-Dessouky et al. [9]	Mistry et al. [10]	Present
Programming method	Sequential	Simultaneous	Simultaneous
Heat transfer area of evaporators	Constant	Constant	Constant
Heat transfer area of preheaters	Constant	Constant	Constant
BPE	Variable	Constant	Variable
NEA	Variable	Neglected	Variable
Non-condensable gases effect	Yes	No	No
Pressure losses	Yes	No	Yes
Tube bundle geometry	Yes	No	No
Thermophysical properties of seawater	Variable	Variable	Variable
Temperature difference between effects	Variable	Variable	Variable
Number of preheaters	$N-2$	$N-1$	$N-1$
Overall heat transfer coefficient	$f(R,h)$	$f(T)$	$f(T)$
Flow rate of vapour condensed in the preheaters	Only flash	Fraction of total vapour	Fraction of total vapour

Fig. 5 shows the GOR and sA simulations as function of the number of effects, along with the results obtained by Mistry et al. [10]. It can be seen how the relative error made is lower than 2% for the GOR and 7% for the sA, following the same trend in both cases. It is observed that when the number of effects is increased, the water productivity (GOR) grows but progressively decreases possibly due to the elevation of the saturation temperature losses of the vapour and the increase of the specific heat of evaporation. Also, the overall heat transfer coefficient associated with the heat exchangers decreases along the effects of the MED plant, which degrades the heat transfer process and reduces the freshwater production. Regarding the sA, a good agreement with Mistry et al. [10] is also found. As shown, the sA increases considerably with the number of effects due to the difference of temperature between effects become smaller and hence the driving force of the evaporation process.

Other significant variable for the assessment of the MED design is the maximum temperature reached by the brine (TBT), which in the case of FF arrangement takes place in the first effect. There is a practical limit for this parameter at nearly 70°C (saturated vapour) due to the appearance of scaling (salts precipitation) on the tubes of the evaporators, which is favoured by the increase of the seawater temperature. Both models are also compared with respect to the GOR and sA by varying the heating steam temperature (T_s, which is equivalent to vary the TBT), with the number of effects fixed to 8 (Fig. 6). As can be seen, the curves obtained using the current model for both parameters present a good agreement with the results obtained by Mistry et al. [10]. The maximum relative errors found are lower than 2% and 8% for the GOR and sA, respectively. It is also observed that the GOR decreases only slightly (9.5%) when the heating steam temperature is elevated from 60°C to 100°C (40%). The decrease on the specific heat transfer area is more considerable, on the contrary.

3.2. Sensitivity analysis

In this section, several key parameters for the design and operation of MED-FF systems, such as number of effects, temperature difference between effects, fraction of steam condensed in the preheaters, mass flow rate of distillate produced in each effect, etc. are analyzed using the developed model. The base case selected for the sensitivity analysis is the one described in Mistry et al. [10], previously defined in section 3.1, but changing the last effect temperature for the

Table 2
Inputs taken for the validation of the model

Parameter	Value
Number of effects	3-19
Fresh water production, kg/s	1
Heating steam temperature, °C	70
Intake seawater temperature, °C	25
Intake seawater salinity, ppm	42,000
Brine blow down temperature, °C	40
Brine blow down salinity, ppm	70,000
Minimum TTD in preheaters, °C	5
Temperature rise in the end condenser, °C	10

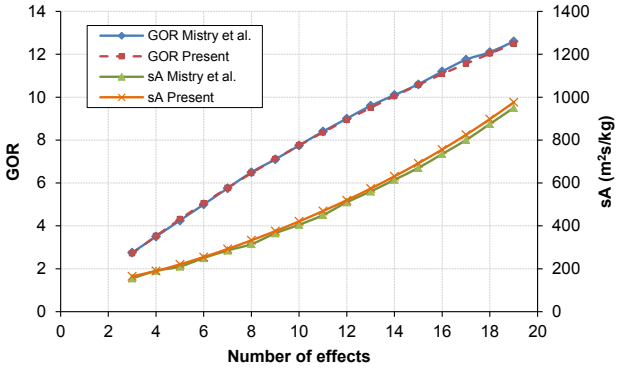

Fig. 5. Comparison of the GOR and sA as function of the number of effects using the model from Mistry et al. [10] and the present one.

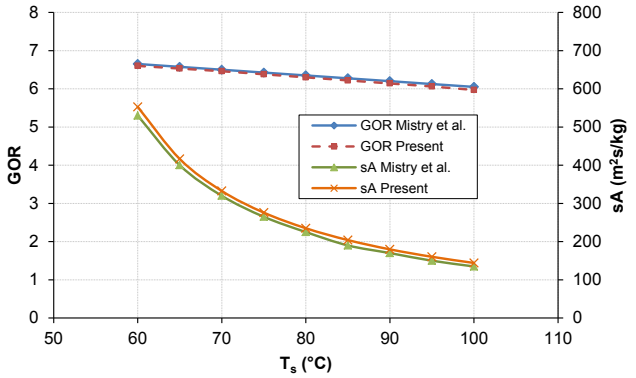

Fig. 6. Comparison of the GOR and sA (specific heat transfer area) as function of the heating steam temperature (T_s) using the model from Mistry et al. [10] and the present one.

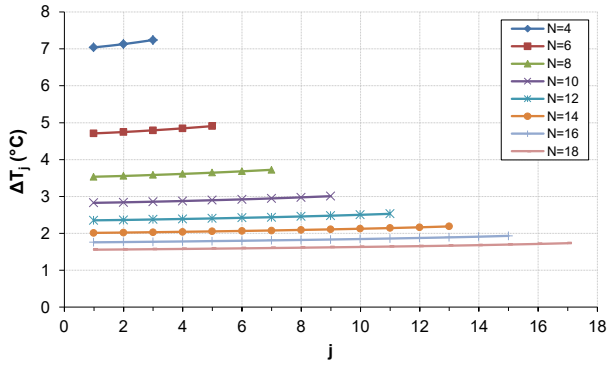

Fig. 7. Difference of temperature between effects for different number of effects, from N = 4 to 18.

terminal temperature difference (TTD) in the end condenser, which is chosen as 5°C. As the temperature increase of the seawater at the end condenser is fixed (10°C), the condensation temperature is also specified to 40°C. Also, the saturation temperature losses of the vapour have been minimized by removing all the demisters except the first one and increasing the diameters of the connecting lines and evaporator tubes.

3.2.1. Temperature difference between effects and preheaters

The difference of temperature between effects is an important parameter for the design of MED units and represents the driven force of the evaporation process in each effect. An increase of the number of effects, maintaining the total temperature difference between effect 1 and effect N constant, produces a decrease of the temperature drop between effects (ΔT_j), as depicted in Fig. 7, and consequently, a significant growth of the specific heat transfer area. Therefore, there is a practical limit in the maximum number of effects in MED plants related to an allowable temperature difference between effects, which usually lies between 2°C and 3°C [21]. Noteworthy, the effective temperature difference should discount the saturation temperature drops of the vapour (generally known as thermodynamic losses) which further limit the practical number of effects. Moreover, the temperature drop profiles along effects show a slight variation for low number of effects. Similar trends are observed for the temperature difference between preheaters, as shown in Fig. 8. It can be seen how the temperature variation decreases with the elevation of the number of effects, and their values are similar to those of the temperature differences between effects. In the particular case simulated, if 3°C is selected as a reasonable value for the temperature difference, the number of effects should be below 10.

3.2.2. Mass fraction of vapour condensed in the preheaters

In this model, it has been assumed that a fraction of the total vapour generated in each effect (by boiling in the evaporator, flash of the sprayed brine and flash of the distillate collected in the flash box), denoted by α, condenses in the outer surface of the tubes in the preheater. The amount of condensed steam is directly associated with the boundary

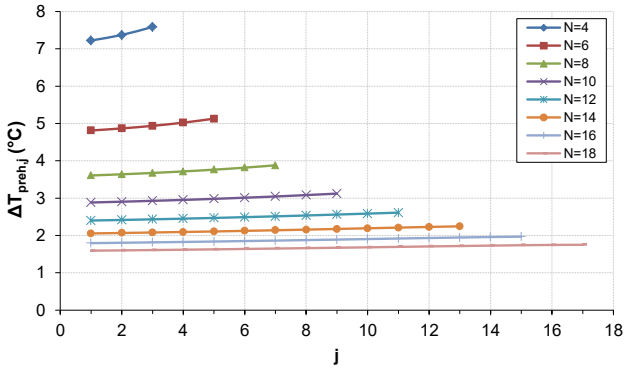

Fig. 8. Difference of temperature between preheaters for different number of effects, from N = 4 to 18.

conditions imposed for solving the model, specifically the level of preheating of the feedwater. In this case, the TTD of the preheater associated with the first effect is fixed to 5°C, which is the difference of temperature between the TBT and the seawater entering the first effect, while for the rest there are not restrictions imposed. Fig. 9 shows how the mass of vapour condensed is higher within the first preheaters and decreases gradually up to the last, possibly due to the lower temperature level of the vapour from the last effects.

3.2.3. Terminal temperature difference of the preheaters

The terminal temperature difference of the preheaters for different number of effects are depicted in Fig. 10, tending to increase along the plant from the minimum value, 5°C, which is reached in the preheater associated with the first effect. These parameters are important because they have a great influence on the temperature of the seawater entering the first effect. The higher this temperature is, the lower thermal consumption needed, due to the less thermal energy required to preheat the seawater up to the saturation temperature. However, the area needed in the heat exchangers increases significantly, so the selection of this parameter should account for this trade-off.

In the base case of study, the TTD of the preheater associated with the first effect was selected to be 5°C, as a

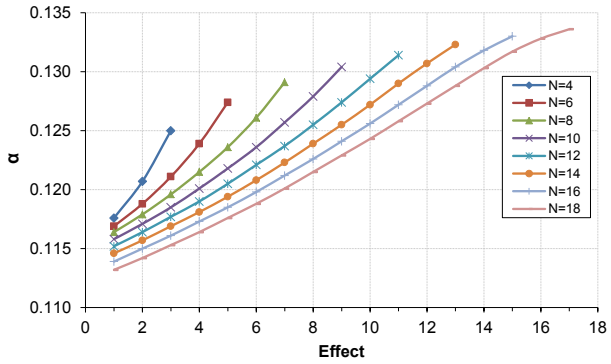

Fig. 9. Fraction of vapour condensed in each preheater as function of the number of effects, from $N = 4$ to 18.

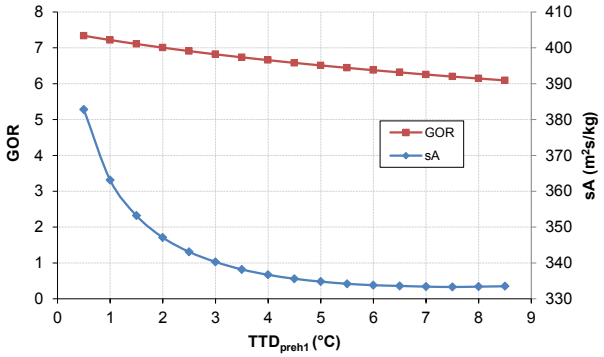

Fig. 11. Gain output ratio and specific heat transfer area as function of the terminal temperature difference at the preheater of the first effect.

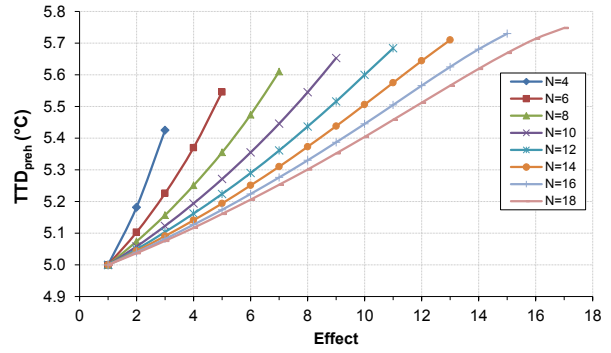

Fig. 10. Terminal temperature difference in the preheaters as function of the number of effects, from $N = 4$ to 18.

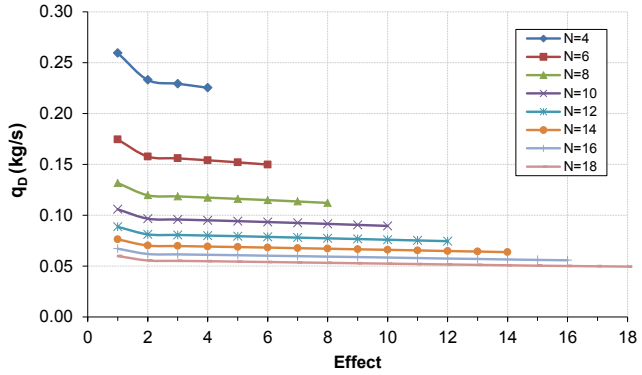

Fig. 12. Mass flow rate of vapour produced by boiling in each effect (q_D), for different number of effects (N).

conservative value (typically ranges from 3°C to 5°C). The effect of the variation of this parameter on the GOR and sA is presented in Fig. 11. As mentioned above, a decrease in the TTD_{preh1} not only improves the GOR but also increases the specific heat transfer area. It is needed a compromise solution between the size of the heat exchanger (and therefore its cost) and the productivity of the plant. For values lower than 4°C–3°C, the specific heat transfer area grows markedly.

3.2.4. Vapour produced by boiling in each effect

The distribution of the mass flow rate of vapour produced by boiling in each effect (q_D), for different number of effects, is depicted in Fig. 12. The vapour produced slightly decreases in each effect, starting from the first. As a first approximation and in the case of high number of effects, the vapour produced in each effect may be considered constant as its variation is small. However, the little decrease could be caused by the increase on the specific enthalpy of evaporation of the seawater and the saturation temperature losses of the vapour along the effects.

3.2.5. Internal diameter of the pipes connecting the effects

In the base case considered, the distillate production has been fixed as 1 kg/s, which is a typical value used in the literature for the analysis of MED models. Nevertheless, it is interesting to investigate the influence of this parameter on the pressure losses of the vapour in the connecting lines between effects, which will eventually affect the water productivity and heat transfer area of evaporators. For this purpose, different internal diameter of the pipes between effects have been considered, from 1,000 to 200 mm, and the distillate production has been varied from 1 to 35 kg/s (nearly 86 and 3,024 m^3/d, respectively), as shown in Fig. 13. As the larger vapour pressure loss inside the pipes of the connecting lines has place on the last effect ($N = 8$), where the vapour is driven to the end condenser, it has been selected for the simulation as the key design parameter. Therefore, Fig. 13 shows the saturation pressure losses of the vapour flowing from the last effect to the end condenser, as function of the total distillate produced, and for different tube diameters. In addition, same features of the base case have been used along with the data presented in Table 3. Also, for this analysis, the presence of all the demisters has been considered and the thermodynamic losses have been accounted.

From Fig. 13, it is concluded that the pressure losses greatly increase with the distillate production when the internal diameter of the connecting lines are lower than 400 mm. In fact, for an internal diameter of 300 mm and a daily production of 3,000 m^3/d, the pressure losses due to friction inside the pipe connecting the last effect and the end condenser are of 2,145 Pa, which produce a saturation temperature drop of the vapour of almost 5°C, as can be seen in Fig. 14. These

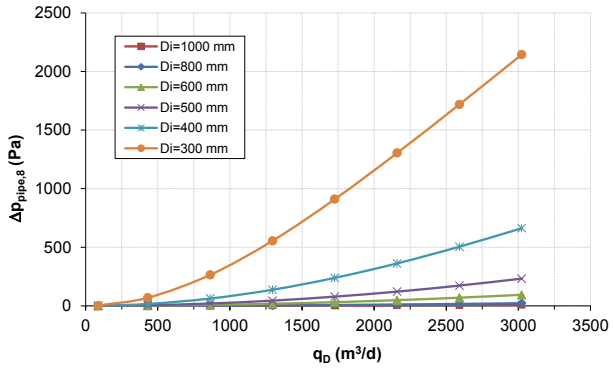

Fig. 13. Pressure drop in the pipe connecting effect 8 and end condenser as function of the distillate production and for different internal diameters.

are unfeasible conditions because the value of the thermodynamic losses in that case would rapidly increase the specific heat transfer area (Fig. 15), due to the decrease on the temperature difference between the condensing vapour inside the evaporator and the boiling brine in the corresponding effect. Typically, the total saturation temperature losses of the vapour may vary in the range of 0.5°C–3°C [22], so the minimum diameter of the pipes connecting the effects should be of 400 mm in this particular case.

3.2.6. Intake seawater salinity

The salinity of the intake seawater is an important design parameter that depends on the location of the plant. Although the mean salinity of the seawater is typically considered as 35 g/L (South Atlantic ocean), some areas of the world present higher salinity values, such as the Red Sea and Persian Gulf region, with seawater salinity of around 40 and 50 g/L, respectively [23]. Therefore, the influence of this parameter on the GOR, sA and specific flow rate of cooling seawater (sq_{cw}), defined as the mass flow rate of cooling seawater divided by the distillate production, has been analyzed and the results are presented in Fig. 16. It can be seen how the GOR and the sq_{cw} decrease with the increase in the intake seawater salinity, while the sA varies slightly reaching a maximum for a specific value of the salinity. The elevation of the intake seawater salinity reduces the recovery ratio, all other variables maintained constant, and therefore increases the feedwater flow rate. Moreover, it decreases the rejected cooling seawater as the distillate production does not vary and the amount of total vapour to be condensed at the end condenser is almost the same. Hence, the intake seawater entering the end condenser does not change significantly. The reduction of the GOR may be explained by lower preheating of the feedwater flow rate, which is importantly reduced due to the increase of the feedwater flow rate. Because of that, the heat added in the first effect must be higher and more heating steam flow rate is consumed.

4. Analysis of the MED process with high heating steam temperature

In this section, it is analyzed the elevation of the heating steam temperature (which is equivalent to increase the

Table 3
Features of demisters, pipes connecting lines and evaporators

Parameter	Value
Length of connecting lines, m	2
Length of evaporator tubes, m	5
External diameter of evaporator tubes, m	0.030
External diameter of evaporator tubes, m	0.029
Wire diameter of demisters, mm	0.28
Density of demisters, kg/m^3	280
Mesh pad thickness of demisters, m	0.15
Diameter of the vessel, m	4.8

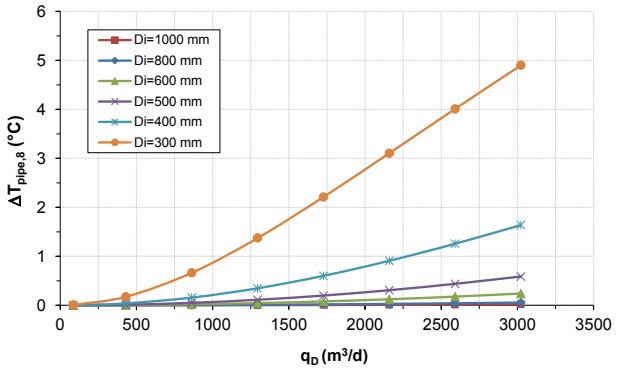

Fig. 14. Saturation temperature decrease of the vapour in the pipe connecting effect 8 and end condenser as function of the distillate production and for different internal diameters of the pipes.

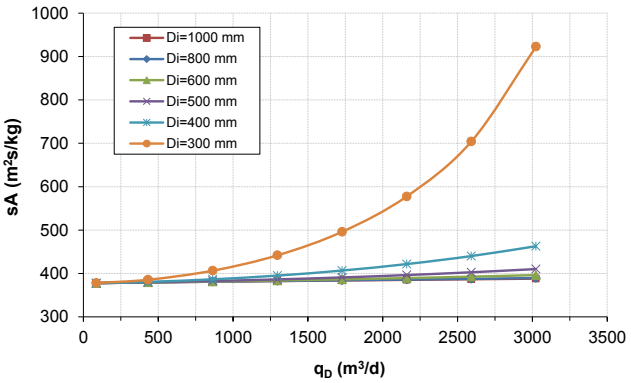

Fig. 15. Specific heat transfer area as function of the distillate production and for different internal diameters of the pipes connecting the effects.

TBT) in order to reach higher water productivity on the MED process. This permits to elevate the number of effects up to a limit imposed by the minimum temperature difference between effects. The simulations have been done with the same inputs that the base case but changing the last effect temperature from 40°C to 35°C and temperature increase of the seawater in the end condenser from 10°C to 7°C. The analysis has been done taken into account mean temperature differences between effects in the range of 2°C–4°C.

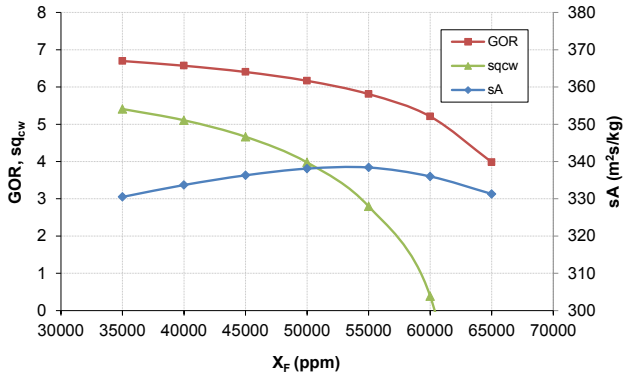

Fig. 16. Gain output ratio, specific heat transfer area and specific flow rate of cooling seawater as function of feed salinity.

The influence of the number of effects, or equivalently, the mean temperature difference between effects (with fixed top and bottom temperatures) on the GOR is analyzed in Fig. 17, for three different heating steam temperatures: 70°C, 100°C and 120°C. It is observed that a decrease in the mean temperature difference between effects, that is, an increase of the number of effects, increases the GOR significantly for every heating steam temperature analyzed, and the elevation is and it grows with the heating steam temperature is. As an example, for a mean temperature difference of 2.5°C, the maximum number of effects for heating steam temperatures of 70°C, 100°C and 120°C are 14, 26 and 34, with GOR 10.38, 15.34 and 17.6, respectively. This figure permits us to obtain the productivity of the MED process depending on the number of effects and heating steam temperature, which is useful in preliminary design of MED plants. It is interesting to note that the maximum GOR reached is about 18, for 34 effects, which could lead to high capital costs. However, the capital cost of the MED plant, mainly associated with the required specific heat transfer area, is analyzed in Fig. 18.

As commented before, when the temperature difference between effects is reduced, for a given heating steam temperature, the specific heat transfer area (and capital costs) rapidly increases. This can be clearly seen in Fig. 18. But if at the same time the heating steam temperature is increased, more effects can be considered with a similar temperature drop, and the corresponding specific heat transfer area is reduced. Particularly, for a temperature difference of 2.5°C, and heating steam temperatures of 70°C, 100°C and 120°C, the resulting number of effects are 14, 26 and 34, with sA of 518.2, 483.1 and 463.9 $m^2/(kg/s)$. The reduction of the specific heat transfer area with the rise of the heating steam temperature, all other variables maintained constant, may be attributed to the improvement in the heat transfer process, specifically higher values of the overall heat transfer coefficients in the evaporators.

Also, for a given freshwater production and heating steam temperature, increasing the number of effects further exploits the thermal energy introduced in the system and reduces the specific thermal energy consumption, sE, as is depicted in Fig. 19. If the mean temperature difference between effects is maintained constant, increasing the heating steam temperature also decreases the specific thermal energy consumption because more effects can be introduced,

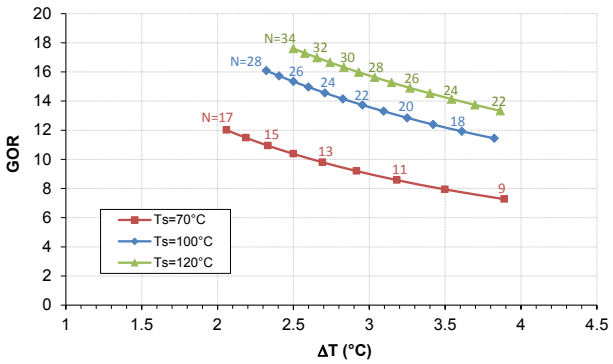

Fig. 17. Gain output ratio as function of the mean temperature difference between effects and the number of effects, for each heating steam temperature.

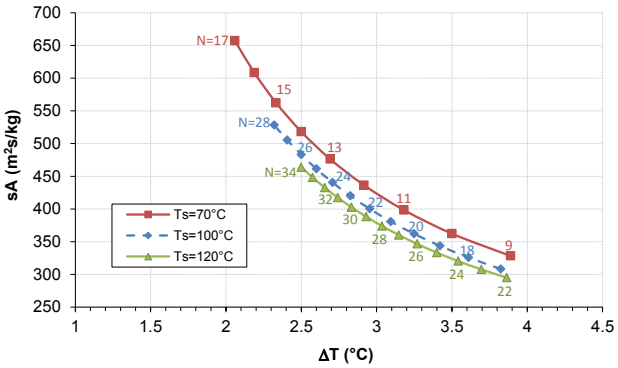

Fig. 18. Specific heat transfer area as function of the mean temperature difference between effects and the number of effects, for each heating steam temperature.

which permits additional reuses of the thermal energy contained in the vapour. For the particular case considered of a difference of temperature of 2.5°C, the sE is 61.98, 40.54 and 34.49 kWh/m^3 for 70°C, 100°C and 120°C, respectively.

In view of these results, the selection of the best design in high temperature FF-MED schemes should be a compromise solution between obtaining higher GOR or, on the contrary, lower specific heat transfer area (capital costs).

5. Conclusions

In this study, the possibilities for improvement of the MED process for seawater desalination have been investigated by rising the TBT up to 120°C, which could be achieved by applying seawater pretreatments such as NF. Particularly, an analysis of the main operational and design parameters, GOR, specific heat transfer area and specific thermal energy consumption has been fully addressed, as function of the number of effects. For this purpose, a detailed MED-FF mathematical model has been developed including the saturation temperature losses of the vapour, and different key design parameters have been also evaluated. From the results obtained, the main conclusions reached are presented.

- Increasing the TBT in a MED-FF process by using a seawater pretreatment that removes the bivalent ions

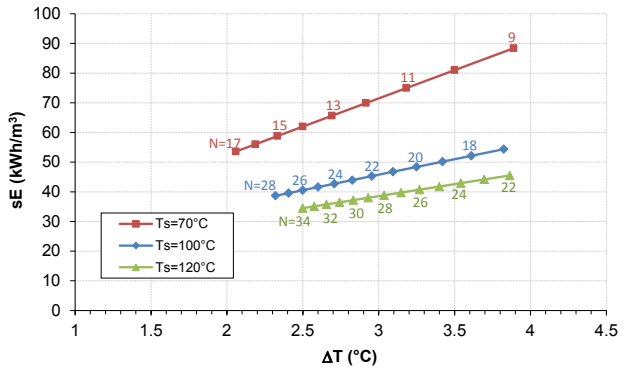

Fig. 19. Specific thermal energy consumption as function of the mean temperature difference between effects and the number of effects, for each heating steam temperature.

(Ca^{2+}, Mg^{2+}, SO_4^{2-}, etc.), for instance based on NF membranes, and for a given mean temperature difference between effects, significantly improves the GOR, decreases the specific heat transfer area and reduces the specific thermal energy consumption. For the particular case study presented, with a mean difference of temperature between effects of 2.5°C, if the heating steam temperature increases from 70°C to 120°C, the GOR improves about 70%, the specific heat transfer area reduces by 11% and the specific thermal energy consumption by 45%.

- For a fixed heating steam temperature, the decrease of the mean temperature difference between effects permits to increase the number of effects, which elevates the GOR but at the expense of greatly increase the specific heat transfer area. For instance, in the case study, to reduce the temperature difference from 3.5°C to 2.5°C with a heating steam temperature of 70°C allows elevating the number of effects from 10 to 14. In this case, the GOR increases nearly 31% (from 7.9 to 10.4), the sA grows by 143% (from 362.4 to 518.2 m^2s/kg) and the sE is reduced by 24% (from 81 to 62 kWh/m^3).
- Effects known in the literature as thermodynamic losses, namely BPE, NEA and saturation temperature losses due to pressure drop in demister, connecting lines and inside the evaporator tubes, considerably increase the specific heat transfer area as they reduce the effective temperature difference between effects. Geometrical features such as internal diameters of the tubes connecting the effects or the length of the tube-bundle of the evaporators are critical. Also, the specific heat transfer area increases with the distillate production because of the augmentation of the saturation temperature losses of the vapour.

This analysis provides insight into the initial design of forward-feed MED plants with seawater pretreatments allowing high-temperature operation, improving the productivity of the process. The trade-off between operation and capital costs, linked to GOR and sA parameters, is a key decision for the feasibility and progressing of MED plants.

Acknowledgement

The authors wish to thank the European Commission (DG for Research & Innovation) for its financial assistance within the Integrated Research Programme in the field of Concentrated Solar Power (CSP) (STAGE-STE Project; Grant Agreement No. 609837).

Symbols

A	—	Heat transfer area, m^2
c	—	Specific heat, kJ/kg °C
h	—	Specific enthalpy, kJ/kg
N	—	Number of effects
q	—	Mass flow rate, kg/s
Q	—	Heat rate, kW
sA	—	Specific heat transfer area, $m^2/(kg/s)$
sE	—	Specific thermal energy consumption, kWh/m^3
sq_{cw}	—	Specific flow rate of cooling seawater
T	—	Temperature, °C
t	—	Temperature of the feedwater, °C
X	—	Salinity, ppm
U	—	Overall heat transfer coefficient, $kW/(m^2\,°C)$
BPE	—	Boiling point elevation, °C
CV	—	Control volume
FF	—	Forward feed
GOR	—	Gain output ratio
LMTD	—	Logarithmic mean temperature difference, °C
NEA	—	Non-equilibrium allowance, °C
MED	—	Multi-effect distillation
MSF	—	Multi-stage flash
NF	—	Nanofiltration
RO	—	Reverse osmosis
TBT	—	Top brine temperature, °C
TDS	—	Total dissolved solids
TTD	—	Terminal temperature difference, °C

Subscripts

B	—	Brine
c	—	Condenser or condensation
cw	—	Rejected cooling seawater
C	—	Condensate
D	—	Distillate
e	—	Evaporator
F	—	Feed
FB	—	Flash box
FE	—	Flash in the effect
in	—	Intake
l	—	Connecting lines
m	—	Demister
N	—	Last effect
p	—	Pressure
preh	—	Preheater
s	—	Heating steam
sat	—	Saturated conditions
T	—	Total
V	—	Vapour

Superscripts

′	—	Vapour conditions after the demister
″	—	Vapour conditions in the flash box

Greek

α — Fraction of vapour condensed
λ — Specific enthalpy of phase change, kJ/kg

References

[1] A.A. Al-Hamzah, C.M. Fellows, A comparative study of novel scale inhibitors with commercial scale inhibitors used in seawater desalination, Desalination, 359 (2015) 22–25.
[2] A.M. Hassan, M.A.K. Al-Sofi, A.S. Al-Amoudi, A.T.M. Jamaluddin, A.M. Farooque, A. Rowaili, A.G.I. Dalvi, N.M. Kither, G.M. Mustafa, I.A.R. Al-Tisan, A new approach to membrane and thermal seawater desalination processes using nanofiltration membranes (Part 1), Desalination, 118 (1998) 35–51.
[3] A.M. Hassan, Process for desalination of saline water, especially sea water, having increased product yield and quality, WO/1999/016714, 1999. Available at: http://www.freepatentsonline.com/WO1999016714.html.
[4] M. Wilf, L. Awerbuch, The Guidebook to Membrane Desalination Technology: Reverse Osmosis, Nanofiltration and Hybrid Systems: Process, Design, Applications and Economics, Balaban Desalination Publications, L'Aquila, Italy, 2007.
[5] O.A. Hamed, Overview of hybrid desalination systems — current status and future prospects, Desalination, 186 (2005) 207–214.
[6] D. Zhou, L. Zhu, Y. Fu, M. Zhu, L. Xue, Development of lower cost seawater desalination processes using nanofiltration technologies — a review, Desalination, 376 (2015) 109–116.
[7] H.T. El-Dessouky, H.M. Ettouney, Fundamentals of Salt Water Desalination, Elsevier, 2002.
[8] Y.M. El-Sayed, R.S. Silver, Chapter 2 – Fundamentals of Distillation, K.S. Spiegler, A.D.K. Laird, Eds., Principles of Desalination, Academic Press, 1980, pp. 55–109.
[9] H. El-Dessouky, I. Alatiqi, S. Bingulac, H. Ettouney, Steady-state analysis of the multiple effect evaporation desalination process, Chem. Eng. Technol., 21 (1998) 437–451.
[10] K.H. Mistry, M.A. Antar, J.H. Lienhard, An improved model for multiple effect distillation, Desal. Wat. Treat., 51 (2013) 807–821.
[11] S.A. Klein, Engineering Equation Solver Software (EES), 2013. Available at: www.fchart.com.
[12] W. Wagner, A. Pruss, The IAPWS formulation 1995 for the thermodynamic properties of ordinary water substance for general and scientific use, J. Phys. Chem. Ref. Data, 31 (2002) 387–535.
[13] M.H. Sharqawy, J.H. Lienhard V, S.M. Zubair, Thermophysical properties of seawater: a review of existing correlations and data, Desal. Wat. Treat., 16 (2010) 354–380.
[14] H.T. El-Dessouky, H.M. Ettouney, Thermodynamic Losses, H.T. El-Dessouky, H.M. Ettouney, Eds., Fundamentals of Salt Water Desalination, Elsevier Science B.V., Amsterdam, 2002, pp. 565–583.
[15] M. L. Nayyar, Piping Handbook, 7th Edition, McGraw-Hill Education, 2002.
[16] Engineering Scientific Data Unit (ESDU), Condensation Inside Tubes : Pressure Drop in Straight Horizontal Tubes. 91023, ESDU International PLC, United Kingdom, 1993.
[17] L. Friedel, Improved Friction Pressure Drop Correlations for Horizontal and Vertical Two-phase Pipe Flow, European Two-Phase Flow Group Meeting, 1979.
[18] H.T. El-Dessouky, H.M. Ettouney, Chapter 2 – Single Effect Evaporation, H.T. El-Dessouky, H.M. Ettouney, Eds., Fundamentals of Salt Water Desalination, Elsevier Science B.V., Amsterdam, 2002, pp. 19–48.
[19] P. Fiorini, E. Sciubba, C. Sommariva, A new formulation for the non-equilibrium allowance in MSF processes, Desalination, 136 (2001) 177–188.
[20] O. Miyatake, K. Murakami, Y. Kawata, T. Fujii, Fundamental experiments with flash evaporation, Heat Transfer Jpn. Res., 2 (1973) 89–100.
[21] A. Cipollina, G. Micale, L. Rizzuti, A critical assessment of desalination operations in Sicily, Desalination, 182 (2005) 1–12.
[22] H.T. El-Dessouky, H.M. Ettouney, Chapter 4 – Multiple Effect Evaporation, H.T. El-Dessouky, H.M. Ettouney, Eds., Fundamentals of Salt Water Desalination, Elsevier Science B.V., Amsterdam, 2002, pp. 147–208.
[23] A.S. Bower, H.D. Hunt, J.F. Price, Character and dynamics of the Red Sea and Persian Gulf outflows, J. Geophys. Res. Oceans, 105 (2000) 6387–6414.